

Article

Adsorption of Mixed Dye System with Cetyltrimethylammonium Bromide Modified Sepiolite: Characterization, Performance, Kinetics and Thermodynamics

Jian Yu ¹, Aiyi Zou ¹, Wenting He ¹ and Bin Liu ^{1,2,*} 

¹ Department of Water Engineering and Science, College of Civil Engineering, Hunan University, Changsha 410082, China; yujian@hnu.edu.cn (J.Y.); zouaiyi@hnu.edu.cn (A.Z.); lgc@hnu.edu.cn (W.H.)

² Department of Chemical Engineering, Process Engineering for Sustainable Systems (ProcESS), KU Leuven, Celestijnenlaan 200F, B-3001 Leuven, Belgium

* Correspondence: ahxclb@163.com

Received: 2 March 2020; Accepted: 28 March 2020; Published: 30 March 2020



Abstract: In this study, sepiolite was modified by calcination (200 °C) and cetyltrimethylammonium bromide (CTMAB) treatment. Though the specific surface area sharply declined, the adsorption amount of Acid Orange II (AO), Reactive Blue (RB), Acid Fuchsin (AR) and their mixed solution were improved. The morphology of modified sepiolite showed a better dispersibility and looser structure. The adsorption performance was highly impacted by the pH condition and adsorbent dosage. The electrostatic attraction of positively charged adsorption sites on the adsorbent surface and the negatively charged anionic dye could enhance the adsorption amount especially under acid condition. The order of preferentially adsorbed dye was AO > RB > AR. The adsorption process was much correlated to the quasi-second-order reaction kinetics. The adsorption amount and equilibrium amount of single dye system, as well as in the mixed system were in accordance with the Langmuir model and extended Langmuir isotherm.

Keywords: anionic dye; cetyltrimethylammonium bromide; sepiolite; two-step modification; adsorption

1. Introduction

Synthetic dyes are common pollutants in industrial wastewater. They are stable, highly soluble and when enter in the water bodies present environmental hazards and potential threats to health [1]. Some of the azo dyes have been found to be carcinogenic, sensitizing and reproductive to humans; some of the triarylmethane dyes are also carcinogenic and have long-term adverse effects in the aquatic environment; some of the anthraquinone dyes are chemically stable and refractory to biodegradable [2–4]. Hence, Acid Orange II (azo dye), Reactive Blue (anthraquinone dye) and Acid Fuchsin (triarylmethane dye) were employed in this study to investigate the various kinds of dye.

The treatment methods for dye-bearing wastewater include physical methods, chemical methods and biological methods [5–11]. Among them, adsorption decolorization is the most effective method [12]. According to the different interaction forces between the adsorbate and the adsorbent, the adsorption can be divided into physical adsorption and chemical adsorption [13]. The physical adsorption is caused by the intermolecular force (Van der Waals force) [14]. Chemical adsorption was caused by the formation of chemical bonds or surface coordination compounds by adsorbate molecules and adsorbents by means of ion exchange, electron transfer and electron pair sharing [15,16].

Sepiolite is a hydrous magnesium silicate with a fibrous cross-section [17,18]. The merits of sepiolite were low thermal conductivity, high salt resistance, non-polluting, environmentally friendly [19]. It has

been widely used in various fields due to the special structural properties and low cost. In China, the sepiolite was presented with two types, hydrothermal type and clay type. The clay type is mainly distributed in Hunan province [17]. The water in sepiolite mainly exists with three forms, adsorbing water, coordinating water and hydroxyl water, in which the adsorption water enters the sepiolite pores, the coordinating water is mainly bound by Mg^{2+} and the hydroxyl water exists as OH group [20]. The structure of sepiolite was greatly impacted by the bound water, especially after heated [21]. The three forms of water are gradually lost and the structure of sepiolite will change differently at various temperatures. Serna et al found that the adsorbed water in the sepiolite pores was mainly lost and the specific surface area of the pores was increased at 25–250 °C, but the structure of the sepiolite is folded when the temperature was higher than 300 °C [22].

The adsorbent generally has the following characteristics, large specific surface area, suitable pore structure and surface structure, high adsorption capacity, no chemically react with the medium, good mechanical strength, etc. [19]. The sepiolite, a fibrous hydrous magnesium silicate, has been widely explored as an adsorbent by two reasons: suitable specific surface area; low price, only 20–30 dollars per ton in China. There are three kinds of adsorption active sites from sepiolite: oxygen atom in silicon tetrahedron, water molecules coordinated with magnesium ions, which can form hydrogen bonds with adsorbate and Si-OH combination, formed after the destruction of Si-O-Si.

In order to further improve the adsorption performance of sepiolite, modifications such as thermal acid treatment, surfactant organic and inorganic modifications have been employed [11]. Mahir Alkan et al found thermally modification at 200, the highest adsorption amount was obtained [23]. A wider temperature range of the sepiolite modification was reported by Jiquan Wang et al [24]. The surfactant modification also attracts researcher's attention. Bulent Armagan et al used an organic modification method of natural sepiolite with cetyltrimethylammonium bromide to investigate its adsorption property for anionic dyes (active black, reactive red, active yellow) [25].

In this study, to improve the adsorption property of sepiolite, a combination of heat and surfactant modification method was applied. To confirm the success of this combined method, unmodified and modified forms of sepiolite were characterized by BET, XRD, XPS, FT-IR and SEM. On the other hand, this study also focused on the adsorption performance and mechanism of mixed dye system with modified sepiolite since the kinetics and thermodynamics of two-component and three-component solution were much more complicated. Hence, the three dyes, Acid Orange II, Reactive Blue and Acid Fuchsin were employed as target adsorbate with single, two-component and three-component solution type.

2. Method and Material

2.1. Materials

In this study, the original sepiolite was obtained from Guangda sepiolite company (Hunan province, China). The three dyes, Acid Orange II (AO), Reactive Blue (RB) and Acid Fuchsin (AR) was purchased from Sigma company and the detail information can be found in previous work [26–28]. The Cetyltrimethylammonium bromide (CTMAB), with the formula of $C_{16}H_{33}(CH_3)_3NBr$, was purchased from Tianjin Bodi Chemical company. The chemical agents were all above analytical grade in this work. To compare the adsorption amount and specific surface area, commercial powder activated carbon (granularity of 180–220 μm) purchased from Xingyuan company (Hunan province, China) was utilized.

2.2. Preparation of Organically Modified Sepiolite

Before the modification process, the sepiolite was first settled and purified, then dried in an oven at 120 °C and sieved with a 100 mesh. The sepiolite was calcined under 200 °C for 2 h in a muffle. Then, the sepiolite was immersed into CTMAB-saturated solution for 8 h. To remove the CTMAB

solution, the modified sepiolite was repeatedly cleaned and settled. Finally, the modified sepiolite was placed into a 60 °C vacuum oven for 24 h.

2.3. Dye Concentration Determination and Adsorption Test

In this study, a multiple linear regression method was used to process the data. When the photometric system satisfied the linear sum of absorbance, the concentration of each component can be obtained by solving linear equations. Suppose dye wastewater contains dyes with n different absorbance components without mutual react. The sum of the absorbance of each single-component dye is the total absorbance of the mixed dye. It is measured at different wavelengths according to Beer-Lambert law. The absorbance of the mixed dye can be expressed by Equation (1).

$$\begin{pmatrix} A_1 \\ A_2 \\ \dots \\ A_n \end{pmatrix} = \begin{pmatrix} k_{11}k_{12}\dots k_{1m} \\ k_{21}k_{22}\dots k_{2m} \\ \dots \\ k_{n1}k_{n2}\dots k_{nm} \end{pmatrix} \begin{pmatrix} C_1 \\ C_2 \\ \dots \\ C_m \end{pmatrix} \quad (1)$$

where A_i and a_i presents the absorbance at λ_i , k_{ij} was the absorption coefficient of the j th component at wavelength λ_i and C_i is the concentration of the i th component in the sample. To determine the concentration of individual dye, the mixed solution was scanned in the wavelength region of 594–474 nm; the results of dye concentration were calculated using MATLAB software.

A lab scale static adsorption experiment was utilized to investigate the adsorption performance of modified sepiolite with the dye system. A beaker with 300 mL target solution was employed in the experiment. The adsorption test was conducted with 2 g/L sepiolite and 200 mg/L dye solution for 240 min under pH value of 1, oscillation rate of 180 r/min and 25 °C. Considering the effect of pH and adsorbent dosage on adsorption performance, pH range from 1 to 9, dosage range from 0.5 to 5 g/L were utilized. For the mixed dye system, for instance, the RB+AO+AR represents mixed dye of 200 mg/L RB, 200 mg/L AO and 200 mg/L AR, the RB+AO represents mixed dye of 200 mg/L RB and 200 mg/L AO. AO (RB + AO + AR) means the concentration of AO in the three-component system.

After the determination of fixed dye, the decolorization percentage and adsorption amount were calculated by Equations (2) and (3).

$$\eta = \frac{(C_0 - C_e)}{C_0} \times 100\% \quad (2)$$

$$q = \frac{(C_0 - C_e)}{m} V \quad (3)$$

where η and q are the percentage of decolorization and adsorption amount of fixed dye, respectively, C_0 and C_e are the initial and final concentration of fixed dye, V is the dye solution volume and m is the weight of the sepiolite. In order to ensure the accuracy of the test data, each group of experiment was repeated at least 3 times.

2.4. Adsorption Kinetics and Thermodynamics

The kinetic characteristics of mixed dye removal with sepiolite adsorption were discussed by using the quasi-first-order and quasi-secondary kinetics models. The mathematical expressions of quasi-first-order and quasi-secondary kinetic models were listed in Equations (4) and (5), respectively [29].

quasi-first-order model

$$\ln(q_e - q_t) = \ln q_e - k_1 t \quad (4)$$

quasi-secondary-order model

$$\left(\frac{1}{q_t}\right) = \frac{1}{k_2 q_e^2} + \frac{1}{q_e} t \quad (5)$$

where q_e and q_t represent the amount of fixed dye adsorbed by the unit mass adsorbent after equilibrium and at the moment t , k_1 and k_2 represent the adsorption rate constant of the quasi-first-order reaction kinetic equation and the quasi-second-order reaction kinetic equation.

The thermodynamics characteristics of dye solution adsorption were discussed by Langmuir linear fitting model. The mathematical expression of the thermodynamics model was listed in Equation (6).

Langmuir linear fitting model

$$\frac{C_e}{q_e} = \frac{1}{q_{\max}K_L} + \frac{C_e}{q_{\max}} \quad (6)$$

where q_e is the balanced amount of adsorption, q_{\max} is the saturated adsorption capacity of a single layer, c_e is the balanced mass concentration of the dye, K_L is the adsorption equilibrium constant in Langmuir linear fitting model.

In the two-component system, the Langmuir fitting model was transformed to Equations (7) and (8) [30,31]. Where the subscript 1 and 2 present component 1 and component 2 in the mixed system. In this extended Langmuir model, the $\frac{C_{e1}}{q_{e1}}$ shows linear correlation with c_{e1} and $\frac{q_{e2}c_{e1}}{q_{e1}}$.

$$\frac{C_{e1}}{q_{e1}} = \frac{1}{q_{\max1}K_{L1}} + \frac{C_{e1}}{q_{\max1}} + \frac{q_{e2}C_{e1}}{q_{e1}q_{\max2}} \quad (7)$$

$$\frac{C_{e2}}{q_{e2}} = \frac{1}{q_{\max2}K_{L2}} + \frac{C_{e2}}{q_{\max2}} + \frac{q_{e1}C_{e2}}{q_{e1}q_{\max2}} \quad (8)$$

In the three-component system, the Langmuir fitting model was transformed to Equations (9)–(11) [30,31]. Where the subscript 1, 2 and 3 present component 1, component 2 and component 3 in the mixed system. In this extended Langmuir model, the $\frac{C_{e1}}{q_{e1}}$ shows linear correlation with C_{e1} , $\frac{q_{e2}C_{e1}}{q_{e1}}$ and $\frac{q_{e3}C_{e1}}{q_{e1}}$.

$$\frac{C_{e1}}{q_{e1}} = \frac{1}{q_{\max1}K_{L1}} + \frac{C_{e1}}{q_{\max1}} + \frac{q_{e2}C_{e1}}{q_{e1}q_{\max2}} + \frac{q_{e3}C_{e1}}{q_{e1}q_{\max3}} \quad (9)$$

$$\frac{C_{e2}}{q_{e2}} = \frac{1}{q_{\max2}K_{L2}} + \frac{C_{e2}}{q_{\max2}} + \frac{q_{e1}C_{e2}}{q_{e2}q_{\max1}} + \frac{q_{e3}C_{e2}}{q_{e2}q_{\max3}} \quad (10)$$

$$\frac{C_{e3}}{q_{e3}} = \frac{1}{q_{\max3}K_{L3}} + \frac{C_{e3}}{q_{\max3}} + \frac{q_{e1}C_{e3}}{q_{e3}q_{\max1}} + \frac{q_{e2}C_{e3}}{q_{e3}q_{\max2}} \quad (11)$$

2.5. Characterization

A Brunner–Emmet–Teller (BET, QuadraSorb SI, Quantachrome, USA) was utilized for the measurement of specific surface area [32]. An X-ray diffraction spectrometer (D8-Advance, Burke, Germany) was employed for X-ray diffraction spectroscopy (XRD) test [33]. The tube pressure was 20 KV, the scanning range was 5–60° and the scanning speed was 0.02°/0.2 s [34]. A Fourier-transform infrared spectrometer (Spectrum One B, Perkin Elmer, USA) was used to detect the Fourier-transform infrared spectroscopy (FT-IR) [33]. A scanning electron microscopy (Quanta 200, FEI, Hillsboro, OR, USA) was employed to observe the feature of modified sepiolite [35].

3. Result and Discussion

3.1. Characterization of Modified Sepiolite

Figure 1a shows that the adsorption capacity of calcined sepiolite and modified sepiolite were much higher than that of sepiolite ore. The adsorption capacity obviously improved from 45.28 mg/g to 74.82 mg/g and 78.66 mg/g after calcination and CTMAB modification, respectively. The previous study had reported that the calcination process at a suitable temperature range could enhance the adsorption

amount of sepiolite, but the enhancement was undermined at too high temperature. Moreover organic modification could further improve the adsorption capacity.

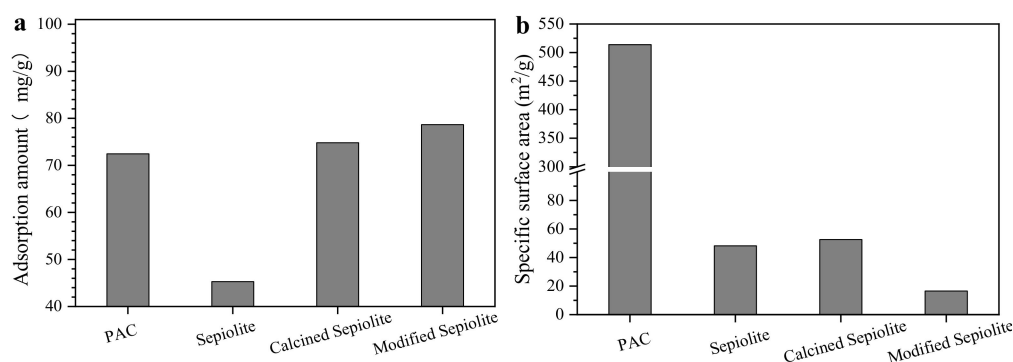


Figure 1. Comparison of Acid Orange II (AO) adsorption amount (a) and specific surface area (b) of different adsorbents.

Figure 1b shows that the specific surface area of calcined sepiolite was slightly increased, but significantly declined after surfactant modification. Though the specific surface area of CTMAB modified sepiolite highly decreased, the adsorption amount was nearly twice when compared to the sepiolite ore. The decrease of electrostatic repulsion of the adsorption site by CTMAB was the reason for adsorption enhancement. Another interesting point was the adsorption amount of organically modified sepiolite was comparable with the powdered activated carbon (PAC), but the specific surface area of PAC was forty times large than the modified sepiolite [36]. This suggests that the specific surface area was not in line with the adsorption capacity, the property of valid adsorption site was the key factor for adsorption performance.

Figure 2a shows that the characteristic dispersion peak of sepiolite at 2θ value of $9.4/9.44$ was significantly strengthened after CTMAB modification and no significant changes occurred at other characteristic peak positions. On the other hand, the diffraction peak of the quartz also enhanced after the surfactant modification, which was different with previous report [34]. The d_{001} value of modified sepiolite was slightly increased to 0.9365 nm, which indicate that the CTMAB intercalated into the sepiolite.

The FT-IR spectrums of original sepiolite, modified sepiolite and modified sepiolite after adsorption saturated are shown in Figure 2b. The 3670 cm^{-1} , 3622 cm^{-1} , 3411 cm^{-1} and 1796 cm^{-1} peaks corresponding to the stretching vibration of O-H bond existed, which reflects the structure of the sepiolite itself. The peak at 3670 cm^{-1} is the stretching vibration of OH (belonging to Mg-OH) which coordinated by the Mg ion octahedron in the sepiolite pore channel. The peak at 3622 cm^{-1} is the crystal water with weak hydrogen bonding and peak at 3411 cm^{-1} is the stretching vibration of the hydroxyl group adsorbing water. The vibration at 1030 cm^{-1} is the stretching vibration of the Si-O group and the absorption band near 796 cm^{-1} , 669 cm^{-1} and 471 cm^{-1} belong to the bending expansion vibration of Si-O and Mg-O in the octahedron. When comparing the spectra of original sepiolite and modified sepiolite, the Si-O and Mg-O stretching vibration peaks of the organically modified sepiolite were enhanced and the peaks at 2920 cm^{-1} , 2856 cm^{-1} and 1420 cm^{-1} appeared [37]. The peaks at 2920 cm^{-1} and 2856 cm^{-1} were corresponding to the stretching vibration of CH_3 and CH_2 from CTMAB, while 1420 cm^{-1} represented the vibration of the C-N. This indicates that cetyltrimethylammonium bromide was electrostatically coated on the surface of sepiolite, which could change the surface of sepiolite from hydrophilic to lipophilic [38]. When comparing the spectra before and after adsorption, the characteristic peak (1500 – 1600 cm^{-1}) of AO appeared on the sepiolite after adsorption, which indicates the surface adsorption distribution occurs during the adsorption process. The XPS spectrum (Figure 2c) shows that the characteristic peaks of Mg and Si decreased while the characteristic peak of C enhanced after CTMAB modification.

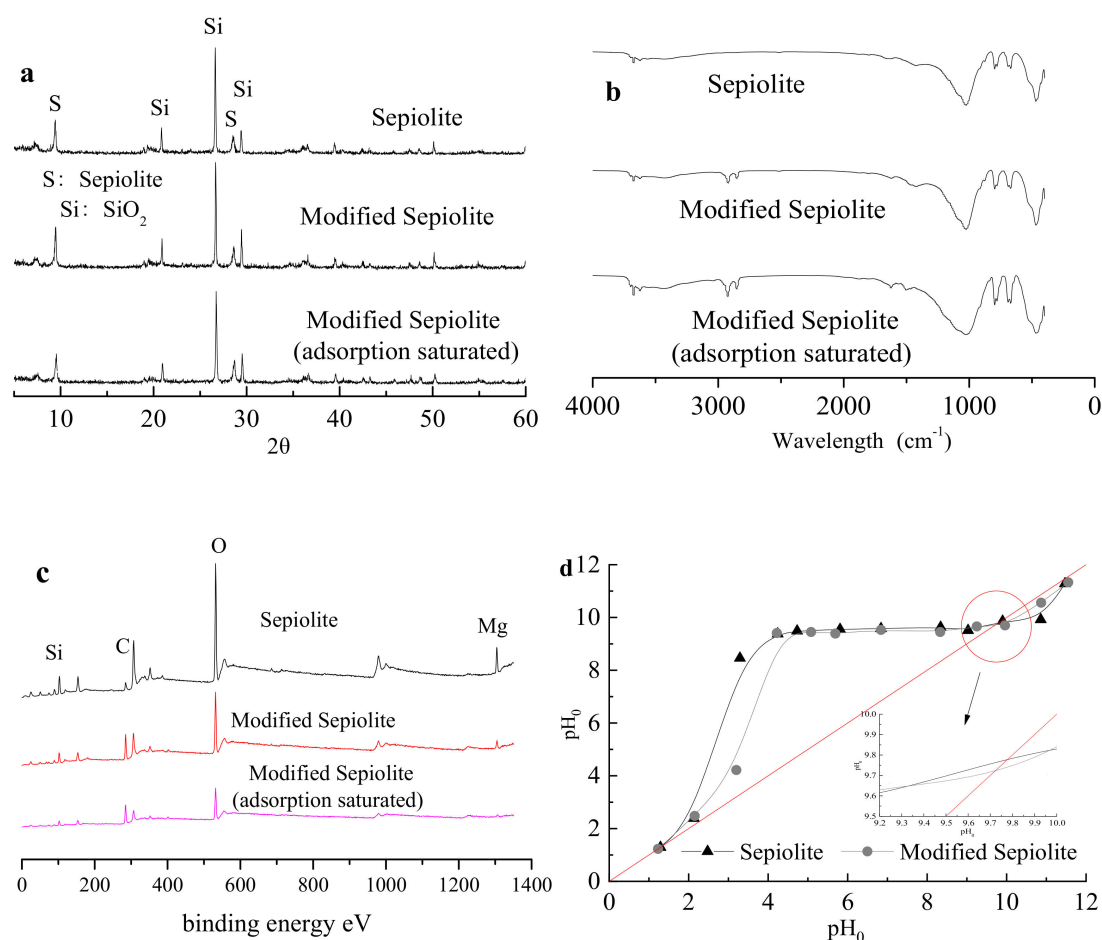
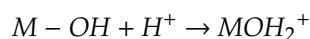


Figure 2. (a) X-ray diffraction spectrum of original sepiolite, modified sepiolite and modified sepiolite after adsorption saturated; (b) Fourier-transform infrared spectrum of original sepiolite, modified sepiolite and modified sepiolite after adsorption saturated; (c) X-ray photoelectron spectrum of original sepiolite, modified sepiolite and modified sepiolite after adsorption saturated; (d) Isoelectric point of original sepiolite and modified sepiolite.

The isoelectric point of the sepiolite before and after the modification was shown in Figure 2d. The isoelectric point changed from 9.62 to 9.87 after modification, which indicates that the isoelectric point value of the surface increased and the surface was positive charged. The isoelectric point is important when investigating the effect of pH on the adsorption effect. When the solution pH is lower than the isoelectric point, the surface of the adsorbent was positively charged. At lower pH condition, the surface of the sepiolite was combined with H^+ and the surface was positively charged, while at higher pH condition, the surface of the sepiolite was combined with OH^- and the surface was negatively charged.



The morphology images confirm that the original crystal structure of the sepiolite was retained after the modification process. Better dispersibility and looser morphology were obtained after modification. The diameter of the fiber increased and the gap between the layered structure was cleaner and smoother (Figure 3a,b).

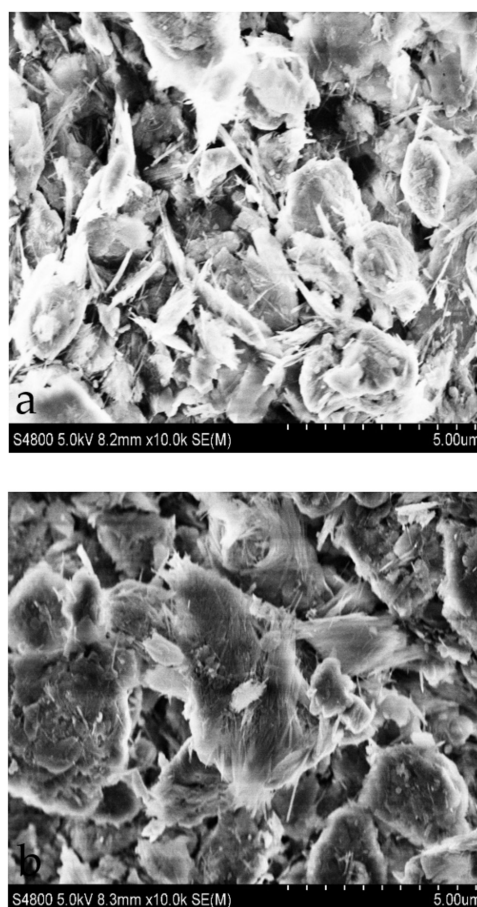


Figure 3. SEM image of original sepiolite (a) and modified sepiolite (b).

3.2. Effect of the Operation Condition on Adsorption Performance

It can be seen from Figure 4a that the removal efficiency of AO and AR by modified sepiolite declined with the increase of pH, which probably because the anionic dye is more protonated under acidic condition [23]. The negatively charged anionic dye could be attracted on the positively charged adsorption sites by electrostatic attraction [39]. When OH^- increased, the anionic dye and OH^- had competitive adsorption [40]. That is also in accordance with the result from Figure 2. In the two-component and three-component mixed solution, the removal efficiency of each dye was basically the same as that of single dye system. The decolorization efficiency of the single component dye in the multi-component system was lower than that of the single dye system. The reduction degree of removal efficiency was $\text{AR} > \text{AO} > \text{RB}$. For instance, the removal efficiency of AR in a single dye system was 96.5%, while reduced to less than 30% in the meta-mixing system and the three-component mixed system.

It can be seen from Figure 4c,d that the removal efficiency of each dye was basically the same during the fixed adsorption condition in single dye system. When the dosage was 3 g/L, the removal efficiency of the three dyes were all 100%. In the mixed dye system, the decolorization behavior of the three dyes was distinct compared to the single dye system. When the dosage of adsorbent was 2 g/L, the decolorization efficiency of AO, RB and AR decreased from 97.48%, 94.49% and 93.6% in the single dye system, to 40.09%, 40.62%, and 15.36% in the three-component system. The decolorization efficiency of AR was rapidly decreased compared with the RB and AO. In the three-component system, when the dosage was lower than 2 g/L, the decolorization efficiency of AO and RB was maintained at the same level and much higher than AR. While the removal efficiency of AO and AR increased rapidly when increasing the adsorbent dosage. This indicates that the AO and RB were preferentially adsorbed.

Moreover, the AO was preferentially adsorbed in the two-component system of AO and RB. The above results indicate that AO had the characteristics of preferential adsorption in the two-component system.

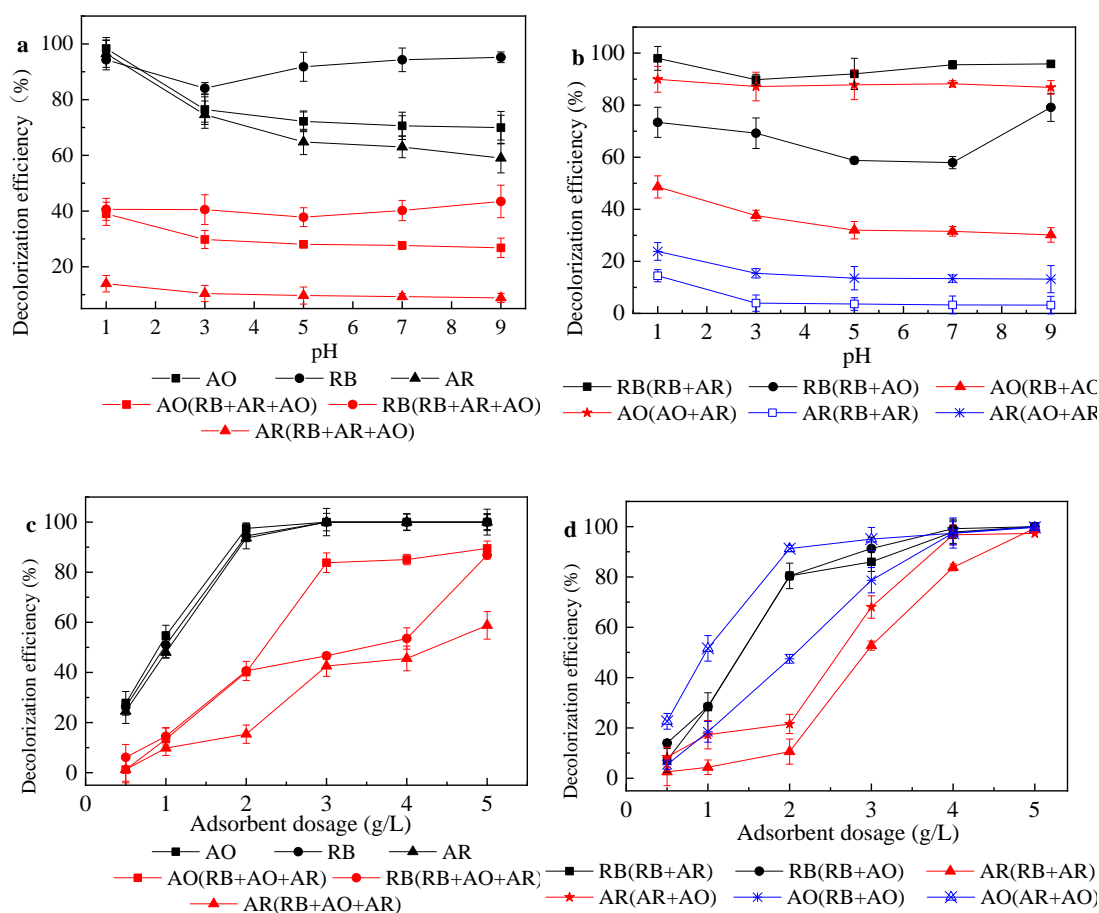


Figure 4. Effect of pH and adsorbent dosage on the Acid Orange II (AO), Reactive Blue (RB) and Acid Red (AR) adsorption performance. In (a) and (b), the adsorption test was conducted with 2 g/L modified sepiolite; In (c) and (d), the adsorption test was conducted under initial pH value of 1.

3.3. Adsorption Kinetics and Thermodynamics

Figure 5a is the kinetic process of the one-component and three-component mixed system. In the single dye system, the adsorption of dyes by the organic modified sepiolite reached equilibrium at 120 min; the adsorption amount of the single dye is sorted as: AO > RB > AR. In the three-component system, the adsorption reaction was also quickly balanced. The rapid reaction of dye and adsorbent may be due to the fact that the total concentration of the anionic dye in the three-component system was larger than the one-component system. On the other hand, the adsorption amount of the three anionic dyes in the three-component mixed system was reduced. Figure 5b is the kinetic curve of the two-component mixed system; the adsorption also reached equilibrium in a short time. The AR appears desorption in the mixed system, which may be because the decrease of the valid sites of the adsorbent after the adsorption reached saturation, while the RB and AO had a competitive advantage and the “substitution effect” occurred [23]. That is, the RB and AO replaced AR from the adsorption site during competitive adsorption.

Since the adsorption kinetics is very fast, most of the experimental data points belong to the steady state, which may skew the mathematical modelling of the adsorption dynamics. It can be seen from Figure 6 that the correlation of the quasi-second-order reaction kinetics fitting was much better than the first-order reaction kinetics fitting; the data in Table 1 also verified. The coefficient of determination of quasi-second-order fitting was between 0.97–0.99, while the coefficient of determination of the

quasi-first-order reaction kinetics was lower than 0.85. The adsorption amount is also consistent with the rate constant, which indicates that the rate constant may have a certain relationship with the adsorption amount. The adsorption rate of the single dye was sorted as AO > RB > AR.

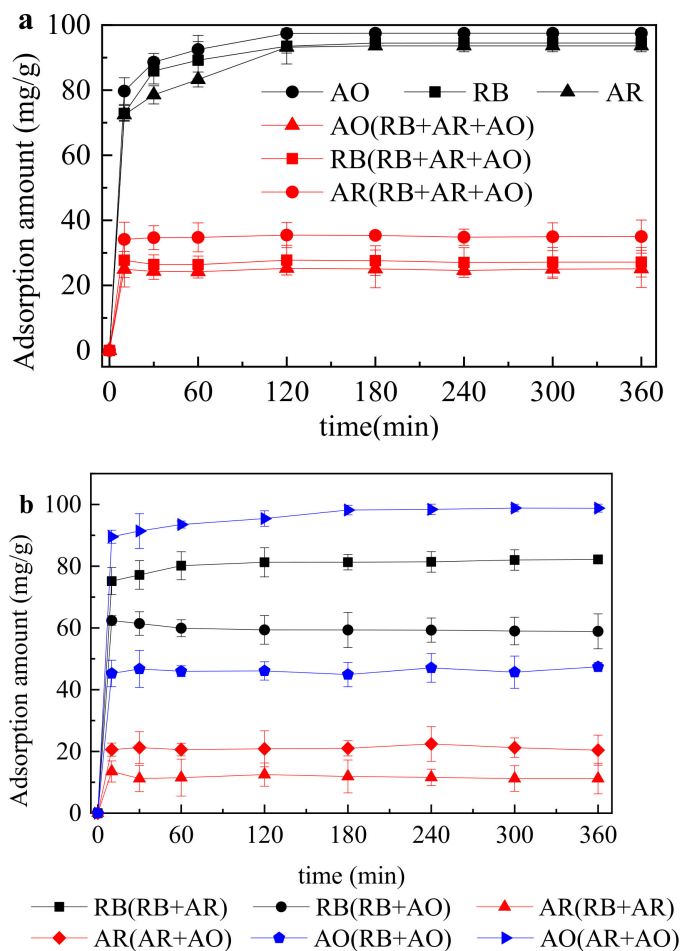


Figure 5. Effect of adsorption duration on the Acid Orange II (AO), Reactive Blue (RB) and Acid Red (AR) adsorption performance. (a) one component and three component system; (b) two component system.

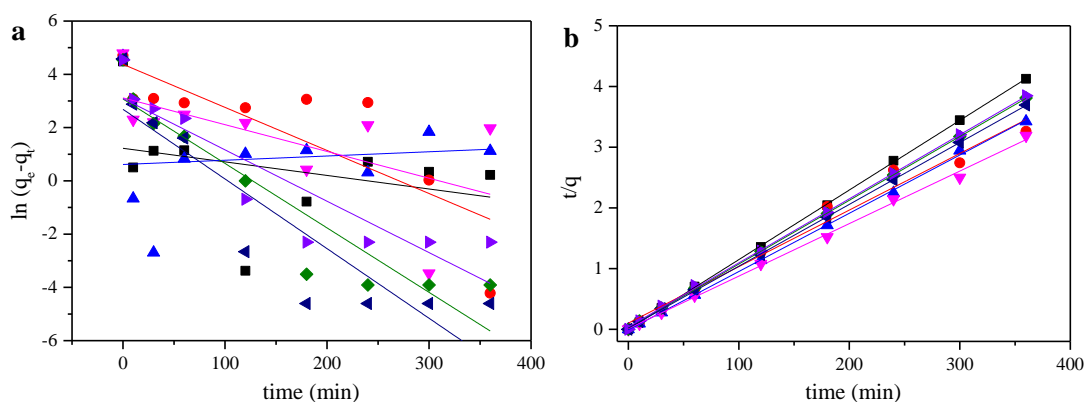


Figure 6. (a) fitting of experimental data with quasi-first-order reaction kinetics; (b) fitting of experimental data with the quasi-second-order model. The adsorption test was conducted with 2 g/L modified sepiolite and 200 mg/L dye solution for 240 min under oscillation rate of 180 r/min and 25 °C.

Table 1. The adsorption kinetics model with various dyes, the adsorption test was conducted with 200 mg/L Acid Orange II and 2 g/L modified sepiolite under oscillation rate of 180 r/min and initial pH value of 1.

| Solution | Quasi-First-Order Reaction Kinetics Model | | | Quasi-Secondary Reaction Kinetics Model | | |
|--------------|---|-----------------------|---------|---|-----------------------|---------|
| | q_{1e} (mg/g) | k_1 (1/min) | R_1^2 | q_{2e} (mg/g) | k_2 (1/min) | R_1^2 |
| RB | 21.62 | 2.42×10^{-2} | 0.85 | 95.24 | 4.53×10^{-3} | 0.99 |
| AO | 14.65 | 2.61×10^{-2} | 0.79 | 98.14 | 5.36×10^{-3} | 0.99 |
| AR | 22.01 | 1.93×10^{-2} | 0.80 | 94.70 | 2.91×10^{-3} | 0.99 |
| RB + AR | 79.46 | 1.61×10^{-2} | 0.61 | 107.30 | 8.6×10^{-2} | 0.97 |
| RB + AO | 1.84 | 1.59×10^{-3} | 0.23 | 104.17 | 1.10×10^{-2} | 0.99 |
| AO + AR | 22.53 | 1.00×10^{-2} | 0.28 | 115.61 | 7.09×10^{-2} | 0.99 |
| RB + AO + AR | 3.39 | 5.09×10^{-3} | 0.56 | 87.18 | 1.42×10^{-1} | 0.99 |

Figure 7 shows the adsorption isotherms of three anionic dyes in single dye systems, two-component and three-component mixed system. In the single dye system, the amount of adsorption increased rapidly as the initial concentration increased until reached saturation and equilibrates. According to the shape of the adsorption isotherm, it is preliminarily determined that the adsorption of the single dye conforms to the Langmuir model; the adsorption of the dye on the sepiolite is single layer adsorption. In the two-component and three-component system, the adsorption isotherm of each dye is not followed a regular Langmuir model [24]. For example, in the three-component mixed system, the adsorption amount of AR and RB decreased with the increase of initial concentration. This trend mainly because of the competitive effect in the adsorption process.

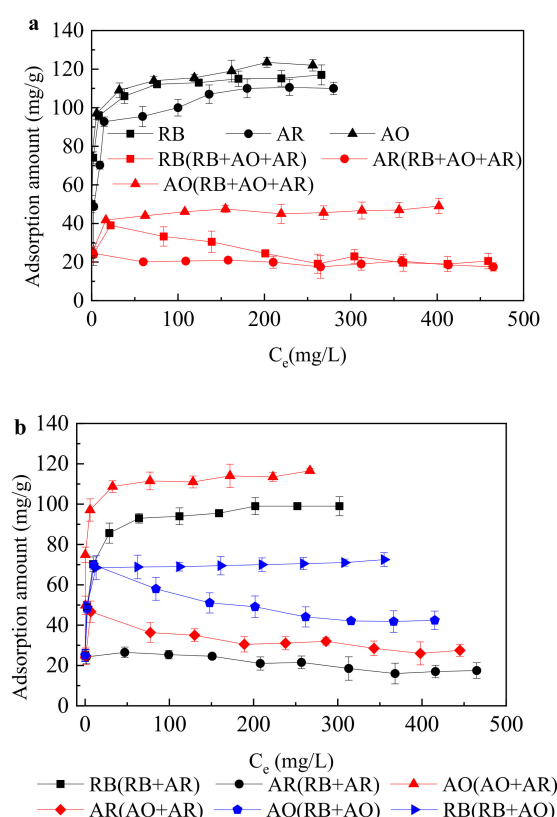


Figure 7. Adsorption isotherm with various dyes. To ensure the adsorbed saturation, the adsorption test was conducted at least 4 h at a certain temperature in a constant temperature oscillating box. (a) one component and three component system; (b) two component system.

Though Langmuir, Freundlich linear fitting model and intraparticle diffusion are the means to discuss the adsorption isotherm, previous work provided that monolayer adsorption was the main adsorption mechanism during and mixed dye adsorption process [30,31]. Hence, the extended Langmuir model was utilized in this study. As can be seen from Table 2, the saturated adsorption capacities of AO, RB and AR were 119 mg/g, 115 mg/g and 110 mg/g, respectively. The adsorption amount of sepiolite to each dye in the mixed system was lower than that from the single system. For instance, when the AO was mixed with RB or AR, its adsorption capacity decreased by 41.2% and 2.1%, and decreased by 58.8% in the three-component mixed system. In the two-component mixed system, the presence of AR had little effect on the adsorption amount of other dyes, and the amount of adsorption itself was minimized in the competitive adsorption process. The decrease of adsorption capacity in the mixed system may have the following factors: the interaction force between the dye solutions, the change of the surface charge of the adsorbent during the adsorption process, the competition of the dye on the active adsorption sites. The adsorption amount and equilibrium amount of single dye system, as well as in the mixed system, were in accordance with the Langmuir model; the coefficient of determination were all over 0.99.

Table 2. Langmuir model fitting results of modified sepiolite adsorption.

| Solution | Langmuir Model | | |
|--------------------|-------------------|--------------|---------|
| | q_{\max} (mg/g) | K_L (L/mg) | R_1^2 |
| RB | 115.0 | 0.32 | 0.99 |
| AO | 119.0 | 0.50 | 0.99 |
| AR | 110.0 | 0.16 | 0.99 |
| RB + AR | 129.9 | 0.34 | 0.99 |
| RB in RB + AR | 107.5 | 0.86 | 0.99 |
| AR in RB + AR | 26.5 | 0.28 | 0.99 |
| RB + AO | 134.9 | 1.55 | 0.99 |
| RB in RB + AO | 72.5 | 2.19 | 0.99 |
| AO in RB + AO | 69.9 | 1.99 | 0.99 |
| AO + AR | 144.9 | 1.00 | 0.99 |
| AO in AO + AR | 116.5 | 3.73 | 0.99 |
| AR in AO + AR | 46.7 | 3.70 | 0.99 |
| RB + AO + AR | 96.2 | 1.85 | 0.99 |
| RB in RB + AO + AR | 39.0 | 0.05 | 0.99 |
| AO in RB + AO + AR | 49.0 | 0.17 | 0.99 |
| AR in RB + AO + AR | 22.7 | 0.04 | 0.99 |

4. Conclusions

In this study, the sepiolite was modified by a two-step method, heat and surfactant modification. The adsorbent was characterized by BET, X-ray diffraction spectroscopy, Fourier-transform infrared spectroscopy and SEM methods. Then the impact of pH and adsorbent dosage on the one-component, two-component and three-component dye system were comprehensively investigated. At last, the kinetics and thermodynamics analysis were studied. The conclusions were listed as follow:

1. The adsorption amounts of Acid Orange II, Reactive Blue and Acid Fuchsin improved after CTMAB modification process, which confirmed the applicability of the modified sepiolite in industrial dye wastewater treatment.
2. The specific surface area of modified sepiolite was obviously decreased, but the adsorption capacity was enhanced. The SEM image shows that the modified sepiolite has a dispersible morphology and the gaps were clean and smooth. The characterization indicate the modification does not deform the sepiolite structure and the CTMAB was successfully loaded.
3. Acid Orange II had the characteristics of preferential adsorption in the two-component system. The electrostatic attraction of positively charged adsorption sites on the adsorbent surface with the negatively charged anionic dye could enhance the adsorption amount under acid condition.

4. The adsorption performance of one-component, two-component and three-component dye system was in accordance with the quasi-second-order reaction kinetics and the adsorption equilibrium time was all around 120 min.
5. The adsorption equilibrium were fitted very well to the Langmuir model and extended Langmuir isotherm.

Author Contributions: Data curation, A.Z. and W.H.; investigation, J.Y.; writing—original draft, B.L. All authors have read and agreed to the published version of the manuscript.

Funding: This research was funded by the special funding for Hunan's innovative province construction (No. 2019SK2111).

Conflicts of Interest: The authors declare no conflict of interest.

References

1. Kolmakov, K.; Hebisch, E.; Wolfram, T.; Nordwig, L.A.; Wurm, C.A.; Ta, H.; Westphal, V.; Belov, V.N.; Hell, S.W. Far-Red Emitting Fluorescent Dyes for Optical Nanoscopy: Fluorinated Silicon-Rhodamines (SiRF Dyes) and Phosphorylated Oxazines. *Chem. A Eur. J.* **2015**, *21*, 13344–13356. [[CrossRef](#)]
2. Singh, R.L.; Singh, P.K.; Singh, R.P. Enzymatic decolorization and degradation of azo dyes—A review. *Int. Biodeterior. Biodegrad.* **2015**, *104*, 21–31. [[CrossRef](#)]
3. Oladipo, A.A.; Gazi, M.; Yilmaz, E. Single and binary adsorption of azo and anthraquinone dyes by chitosan-based hydrogel: Selectivity factor and Box-Behnken process design. *Chem. Eng. Res. Des.* **2015**, *104*, 264–279. [[CrossRef](#)]
4. Baptista, M.S.; Indig, G.L. Effect of BSA Binding on Photophysical and Photochemical Properties of Triarylmethane Dyes. *J. Phys. Chem. B* **1998**, *102*, 4678–4688. [[CrossRef](#)]
5. Robinson, T.; McMullan, G.; Marchant, R.; Nigam, P.; McMullan, G. Remediation of dyes in textile effluent: A critical review on current treatment technologies with a proposed alternative. *Bioresour. Technol.* **2001**, *77*, 247–255. [[CrossRef](#)]
6. Ghoreishi, S.; Haghghi, R. Chemical catalytic reaction and biological oxidation for treatment of non-biodegradable textile effluent. *Chem. Eng. J.* **2003**, *95*, 163–169. [[CrossRef](#)]
7. Demirbas, A. Agricultural based activated carbons for the removal of dyes from aqueous solutions: A review. *J. Hazard. Mater.* **2009**, *167*, 1–9. [[CrossRef](#)] [[PubMed](#)]
8. Shao, S.; Fu, W.; Li, X.; Shi, D.; Jiang, Y.; Li, J.; Gong, T.; Li, X. Membrane fouling by the aggregations formed from oppositely charged organic foulants. *Water Res.* **2019**, *159*, 95–101. [[CrossRef](#)] [[PubMed](#)]
9. Yu, J.; Zhang, D.; Ren, W.; Liu, B. Transport of *Enterococcus faecalis* in granular activated carbon column: Potential energy, migration, and release. *Colloids Surf. B Biointerfaces* **2019**, *183*, 110415. [[CrossRef](#)] [[PubMed](#)]
10. Li, G.; Zhou, S.; Shi, Z.; Meng, X.; Li, L.; Liu, B. Electrochemical degradation of ciprofloxacin on BDD anode using a differential column batch reactor: Mechanisms, kinetics and pathways. *Environ. Sci. Pollut. Res.* **2019**, *26*, 17740–17750. [[CrossRef](#)] [[PubMed](#)]
11. Li, G.; Liu, B.; Bai, L.; Shi, Z.; Tang, X.; Wang, J.; Liang, H.; Zhang, Y.; Van Der Bruggen, B. Improving the performance of loose nanofiltration membranes by poly-dopamine/zwitterionic polymer coating with hydroxyl radical activation. *Sep. Purif. Technol.* **2020**, *238*, 116412. [[CrossRef](#)]
12. Garg, V.; Gupta, R.; Yadav, A.B.; Kumar, R. Dye removal from aqueous solution by adsorption on treated sawdust. *Bioresour. Technol.* **2003**, *89*, 121–124. [[CrossRef](#)]
13. Abbas, A.; Al-Amer, A.M.; Laoui, T.; Al-Marri, M.J.; Nasser, M.S.; Khraisheh, M.; Atieh, M. Heavy metal removal from aqueous solution by advanced carbon nanotubes: Critical review of adsorption applications. *Sep. Purif. Technol.* **2016**, *157*, 141–161.
14. Tillotson, M.J.; Brett, P.; Bennett, R.; Grau-Crespo, R. Adsorption of organic molecules at the TiO₂(110) surface: The effect of van der Waals interactions. *Surf. Sci.* **2015**, *632*, 142–153. [[CrossRef](#)]
15. Song, J.; Xu, T.; Gordin, M.L.; Wang, D. Nitrogen-Doped Mesoporous Carbon Promoted Chemical Adsorption of Sulfur and Fabrication of High-Areal-Capacity Sulfur Cathode with Exceptional Cycling Stability for Lithium-Sulfur Batteries. *Adv. Funct. Mater.* **2014**, *24*, 1243–1250. [[CrossRef](#)]

16. Grassi, M.; Rizzo, L.; Farina, A. Endocrine disruptors compounds, pharmaceuticals and personal care products in urban wastewater: Implications for agricultural reuse and their removal by adsorption process. *Environ. Sci. Pollut. Res.* **2013**, *20*, 3616–3628. [[CrossRef](#)]
17. Wang, Z.; Liao, L.; Hursthouse, A.S.; Song, N.; Ren, B. Sepiolite-Based Adsorbents for the Removal of Potentially Toxic Elements from Water: A Strategic Review for the Case of Environmental Contamination in Hunan, China. *Int. J. Environ. Res. Public Health* **2018**, *15*, 1653. [[CrossRef](#)]
18. Fayazi, M.; Afzali, D.; Ghanei-Motlagh, R.; Iraj, A. Synthesis of novel sepiolite-iron oxide-manganese dioxide nanocomposite and application for lead(II) removal from aqueous solutions. *Environ. Sci. Pollut. Res.* **2019**, *26*, 18893–18903. [[CrossRef](#)]
19. Zaini, N.A.M.; Ismail, H.; Rusli, A. Short Review on Sepiolite-Filled Polymer Nanocomposites. *Polym. Plast. Technol. Eng.* **2017**, *56*, 1665–1679. [[CrossRef](#)]
20. Kara, M.; Yuzer, H.; Sabah, E.; Çelik, M.S. Adsorption of cobalt from aqueous solutions onto sepiolite. *Water Res.* **2003**, *37*, 224–232. [[CrossRef](#)]
21. Chen, Q.; Zhu, R.; Liu, S.; Wu, D.; Fu, H.; Zhu, J.; He, H. Self-templating synthesis of silicon nanorods from natural sepiolite for high-performance lithium-ion battery anodes. *J. Mater. Chem. A* **2018**, *6*, 6356–6362. [[CrossRef](#)]
22. Serna, C.; Vanscoyoc, G. Infrared study of sepiolite and palygorskite surfaces. In *Developments in Sedimentology*; Elsevier: Amsterdam, The Netherlands, 1979; pp. 197–206.
23. Alkan, M.; Demirbas, O.; Çelikçapa, S.; Doğan, M. Sorption of acid red 57 from aqueous solution onto sepiolite. *J. Hazard. Mater.* **2004**, *116*, 135–145. [[CrossRef](#)] [[PubMed](#)]
24. Wang, J.; Wang, D.; Zhang, G.; Guo, Y.; Liu, J. Adsorption of rhodamine B from aqueous solution onto heat-activated sepiolite. *Wuhan Univ. J. Nat. Sci.* **2013**, *18*, 219–225. [[CrossRef](#)]
25. Armağan, B.; Ozdemir, O.; Turan, M.; Celik, M.S. Adsorption of Negatively Charged Azo Dyes onto Surfactant-Modified Sepiolite. *J. Environ. Eng.* **2003**, *129*, 709–715. [[CrossRef](#)]
26. Yu, J.; He, W.; Liu, B. Adsorption of Acid Orange II with Two Step Modified Sepiolite: Optimization, Adsorption Performance, Kinetics, Thermodynamics and Regeneration. *Int. J. Environ. Res. Public Health* **2020**, *17*, 1732. [[CrossRef](#)]
27. Zhang, L.; Zhou, X.; Guo, X.; Song, X.; Liu, X. Investigation on the degradation of acid fuchsin induced oxidation by MgFe₂O₄ under microwave irradiation. *J. Mol. Catal. A Chem.* **2011**, *335*, 31–37. [[CrossRef](#)]
28. Özcan, A.; Ömeroğlu, Ç.; Erdoğan, Y.; Özcan, A.S. Modification of bentonite with a cationic surfactant: An adsorption study of textile dye Reactive Blue 19. *J. Hazard. Mater.* **2007**, *140*, 173–179. [[CrossRef](#)]
29. Yang, X.; Yi, H.; Tang, X.; Zhao, S.; Yang, Z.; Ma, Y.; Feng, T.; Cui, X. Behaviors and kinetics of toluene adsorption-desorption on activated carbons with varying pore structure. *J. Environ. Sci.* **2018**, *67*, 104–114. [[CrossRef](#)]
30. Kurniawan, A.; Sutiono, H.; Indraswati, N.; Ismajji, S. Removal of basic dyes in binary system by adsorption using rarasaponin-bentonite: Revisited of extended Langmuir model. *Chem. Eng. J.* **2012**, *189–190*, 264–274. [[CrossRef](#)]
31. Zhang, Y.-Z.; Li, J.; Zhao, J.; Bian, W.; Li, Y.; Wang, X.-J. Adsorption behavior of modified Iron stick yam skin with Polyethyleneimine as a potential biosorbent for the removal of anionic dyes in single and ternary systems at low temperature. *Bioresour. Technol.* **2016**, *222*, 285–293. [[CrossRef](#)]
32. Oliveira, L.C.; Petkowicz, D.I.; Smaniotto, A.; Pergher, S. Magnetic zeolites: A new adsorbent for removal of metallic contaminants from water. *Water Res.* **2004**, *38*, 3699–3704. [[CrossRef](#)] [[PubMed](#)]
33. Nayak, P.S.; Singh, B.K. Instrumental characterization of clay by XRF, XRD and FTIR. *Bull. Mater. Sci.* **2007**, *30*, 235–238. [[CrossRef](#)]
34. Yu, J.; Zhang, L.; Liu, B. Adsorption of Malachite Green with Sodium Dodecylbenzene Sulfonate Modified Sepiolite: Characterization, Adsorption Performance and Regeneration. *Int. J. Environ. Res. Public Health* **2019**, *16*, 3297. [[CrossRef](#)] [[PubMed](#)]
35. Liu, B.; Qu, F.; Yu, H.; Tian, J.; Chen, W.; Liang, H.; Li, G.; Van Der Bruggen, B. Membrane Fouling and Rejection of Organics during Algae-Laden Water Treatment Using Ultrafiltration: A Comparison between in Situ Pretreatment with Fe(II)/Persulfate and Ozone. *Environ. Sci. Technol.* **2018**, *52*, 765–774. [[CrossRef](#)]
36. Shao, S.; Liang, H.; Qu, F.; Li, K.; Chang, H.; Yu, H.; Li, G. Combined influence by humic acid (HA) and powdered activated carbon (PAC) particles on ultrafiltration membrane fouling. *J. Membr. Sci.* **2016**, *500*, 99–105. [[CrossRef](#)]

37. Tunç, S.; Duman, O.; Çetinkaya, A. Electrokinetic and rheological properties of sepiolite suspensions in the presence of hexadecyltrimethylammonium bromide. *Colloids Surf. A Physicochem. Eng. Asp.* **2011**, *377*, 123–129. [[CrossRef](#)]
38. Yan, L.; Qin, L.-L.; Yu, H.-Q.; Li, S.; Shan, R.-R.; Du, B. Adsorption of acid dyes from aqueous solution by CTMAB modified bentonite: Kinetic and isotherm modeling. *J. Mol. Liq.* **2015**, *211*, 1074–1081. [[CrossRef](#)]
39. Habish, A.J.; Lazarević, S.; Janković-Častvan, I.; Jokić, B.; Kovač, J.; Rogan, J.; Janačković, Đ.; Petrović, R. Nanoscale zerovalent iron (nZVI) supported by natural and acid-activated sepiolites: The effect of the nZVI/support ratio on the composite properties and Cd²⁺ adsorption. *Environ. Sci. Pollut. Res.* **2016**, *24*, 628–643. [[CrossRef](#)]
40. Dashamiri, S.; Ghaedi, M.; Asfaram, A.; Zare, F.; Wang, S. Multi-response optimization of ultrasound assisted competitive adsorption of dyes onto Cu (OH)₂-nanoparticle loaded activated carbon: Central composite design. *Ultrason. Sonochem.* **2017**, *34*, 343–353. [[CrossRef](#)]



© 2020 by the authors. Licensee MDPI, Basel, Switzerland. This article is an open access article distributed under the terms and conditions of the Creative Commons Attribution (CC BY) license (<http://creativecommons.org/licenses/by/4.0/>).